Supplement of Hydrol. Earth Syst. Sci., 29, 3203–3225, 2025
https://doi.org/10.5194/hess-29-3203-2025-supplement

Hydrology and Earth System Sciences
Open Access
EGU

Supplement of

Probabilistic analysis of future drought propagation, persistence, and spatial concurrence in monsoon-dominant Asian regions under climate change

Dineshkumar Muthuvel and Xiaosheng Qin

Correspondence to: Xiaosheng Qin (xsqin@ntu.edu.sg)

Table Caption List

Table S1: Eight possible scenarios of inter-seasonal droughts defined by trivariate joint probabilities

Figure Caption List

Figure S1: Monthly comparison of observed and ensembled historical GCM soil moisture data across four demarcated regions.

Figure S2: Monthly comparison of observed, ensembled, and individual climate model historical precipitation data across four demarcated regions. Grid-wise analysis shows that some models overestimate or underestimate values, with lower weights assigned to such models using Bayesian Model Average (BMA).

Figure S3: Monthly comparison of observed, ensembled, and individual climate model historical soil moisture data across four demarcated regions. Models with significant overestimation or underestimation are assigned lower weights through Bayesian Model Average (BMA).

Figure S4: (a) Monthly distribution of the mean difference between GCM data (Multi-Model Mean using Bayesian Model Averaging) and GLDAS (Observed data) for precipitation and soil moisture, (b) Monthly median of observed precipitation and soil moisture data across four demarcated regions.

Figure S5: Differences in cumulative drought severities between the observed and historical MME for (a) meteorological and (b) agricultural droughts in the period between 1975-2014. Cumulative severity is the sum of index values below -0.5 in the period between 1975-2014 for each grid.

Figure S6: The percentage of drought-affected areas (based on the percentage of grids falling at different ranges of SPI and SSI values) annually. Spatial maps of 2009 drought events.

Figure S7: Spatial maps of propagation durations (timescale, TS) across different seasons and timeframes.

Figure S8: Performance evaluation (RMSE values) of Random Forest (RF) models for each grid across timeframes.

Figure S9: Maps showing the most important variable (highest importance value in a Random Forest model) across timeframes in the study area.

Figure S10: Climate zones based on the Köppen-Geiger climate classification (Kottek et al., 2006)

Figure S11: Spatial concurrent return period between region pairs involving TIB across timeframes. The random variables (percentage of area under drought annually) are shown as black dots.

Figure S12: Correlation between temperature and soil moisture during monsoon season

Table S1: Eight possible scenarios of inter-seasonal droughts defined by trivariate joint probabilities

Scenario	Joint probabilities	Remarks
1	$P(SSI_{Pre-Monsoon} \leq i, SSI_{Monsoon} \leq i, SSI_{Post-Monsoon} \leq i) = \{C(F(i), G(i), H(i))\}$	Persistent all-season droughts
2	$P(SSI_{Pre-Monsoon} \geq i, SSI_{Monsoon} \leq i, SSI_{Post-Monsoon} \leq i) = \{C(G(i), H(i)) - C(F(i), G(i), H(i))\}$	Monsoon and post-monsoon droughts
3	$P(SSI_{Pre-Monsoon} \leq i, SSI_{Monsoon} \leq i, SSI_{Post-Monsoon} \geq i) = \{C(F(i), G(i)) - C(F(i), G(i), H(i))\}$	Pre-monsoon and monsoon droughts
4	$P(SSI_{Pre-Monsoon} \geq i, SSI_{Monsoon} \leq i, SSI_{Post-Monsoon} \geq i) = \{G(i) - C(F(i), G(i)) - C(G(i), H(i)) + C(F(i), G(i), H(i))\}$	Isolated monsoon droughts
5	$P(SSI_{Pre-Monsoon} \leq i, SSI_{Monsoon} \geq i, SSI_{Post-Monsoon} \leq i) = \{C(F(i), H(i)) - C(F(i), G(i), H(i))\}$	Pre-monsoon and post-monsoon droughts
6	$P(SSI_{Pre-Monsoon} \geq i, SSI_{Monsoon} \geq i, SSI_{Post-Monsoon} \leq i) = \{H(i) - C(F(i), H(i)) - C(G(i), H(i)) + C(F(i), G(i), H(i))\}$	Isolated post-monsoon droughts
7	$P(SSI_{Pre-Monsoon} \leq i, SSI_{Monsoon} \geq i, SSI_{Post-Monsoon} \geq i) = \{F(i) - C(F(i), G(i)) - C(F(i), H(i)) + C(F(i), G(i), H(i))\}$	Isolated pre-monsoon droughts
8	$P(SSI_{Pre-Monsoon} \geq i, SSI_{Monsoon} \geq i, SSI_{Post-Monsoon} \geq i) = \{1 - F(i) - G(i) - H(i) + C(F(i), G(i)) + C(F(i), H(i)) + C(G(i), H(i)) - C(F(i), G(i), H(i))\}$	Above-normal wet season annually.

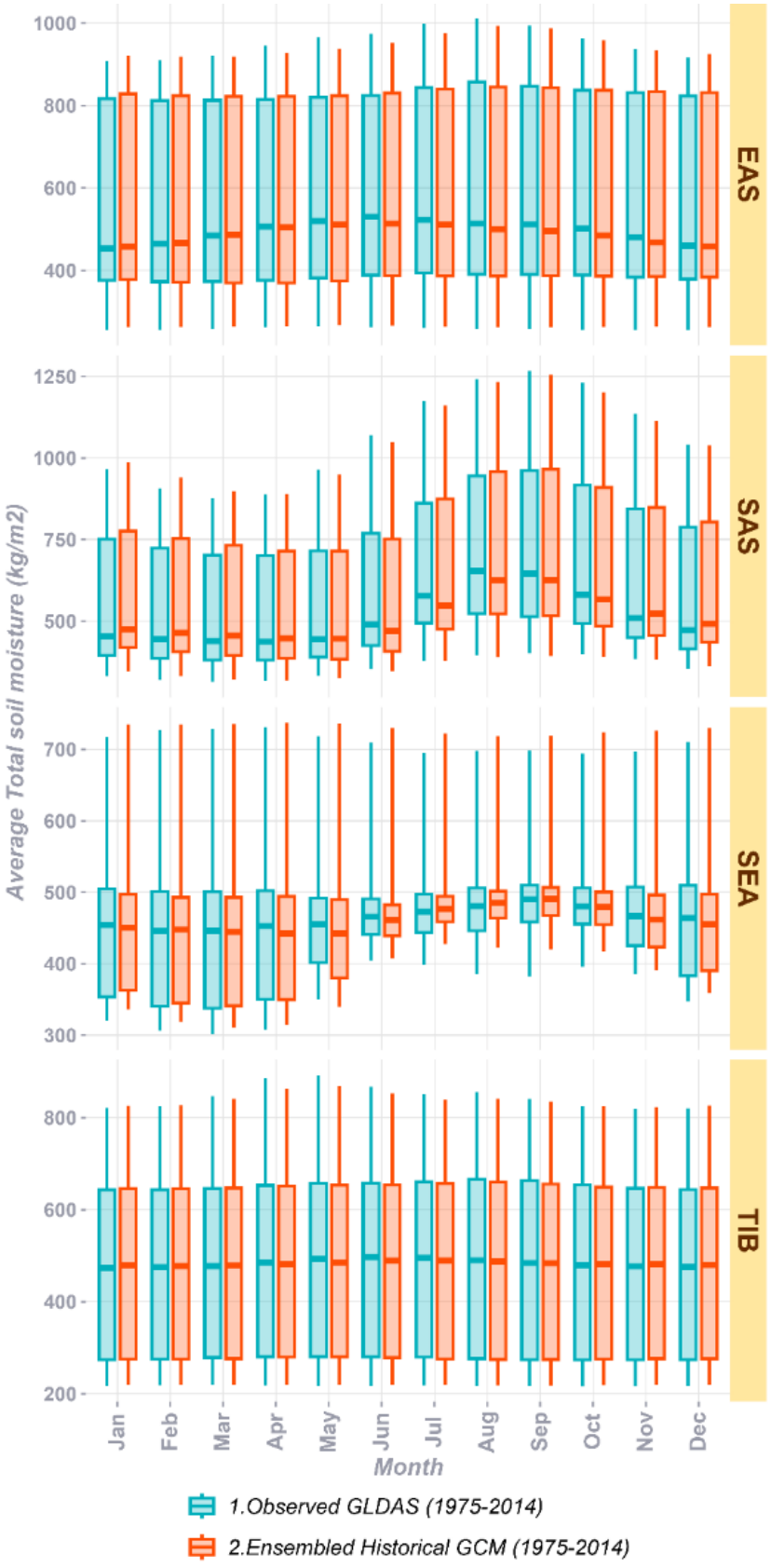

Figure S1: Monthly comparison of observed and ensembled historical GCM soil moisture data across four demarcated regions.

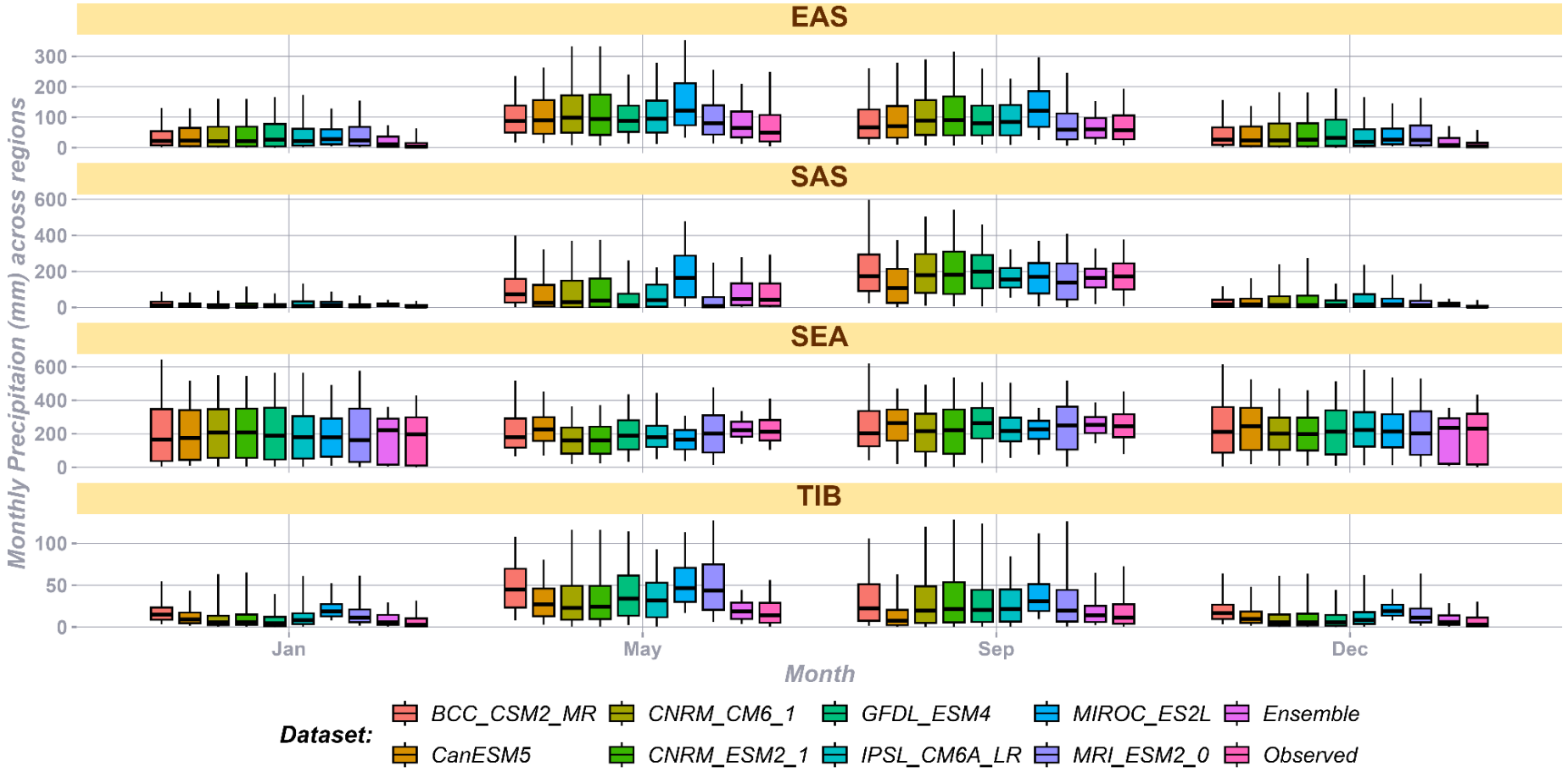

Figure S2: Monthly comparison of observed, ensembled, and individual climate model historical precipitation data across four demarcated regions. Grid-wise analysis shows that some models overestimate or underestimate values, with lower weights assigned to such models using Bayesian Model Average (BMA).

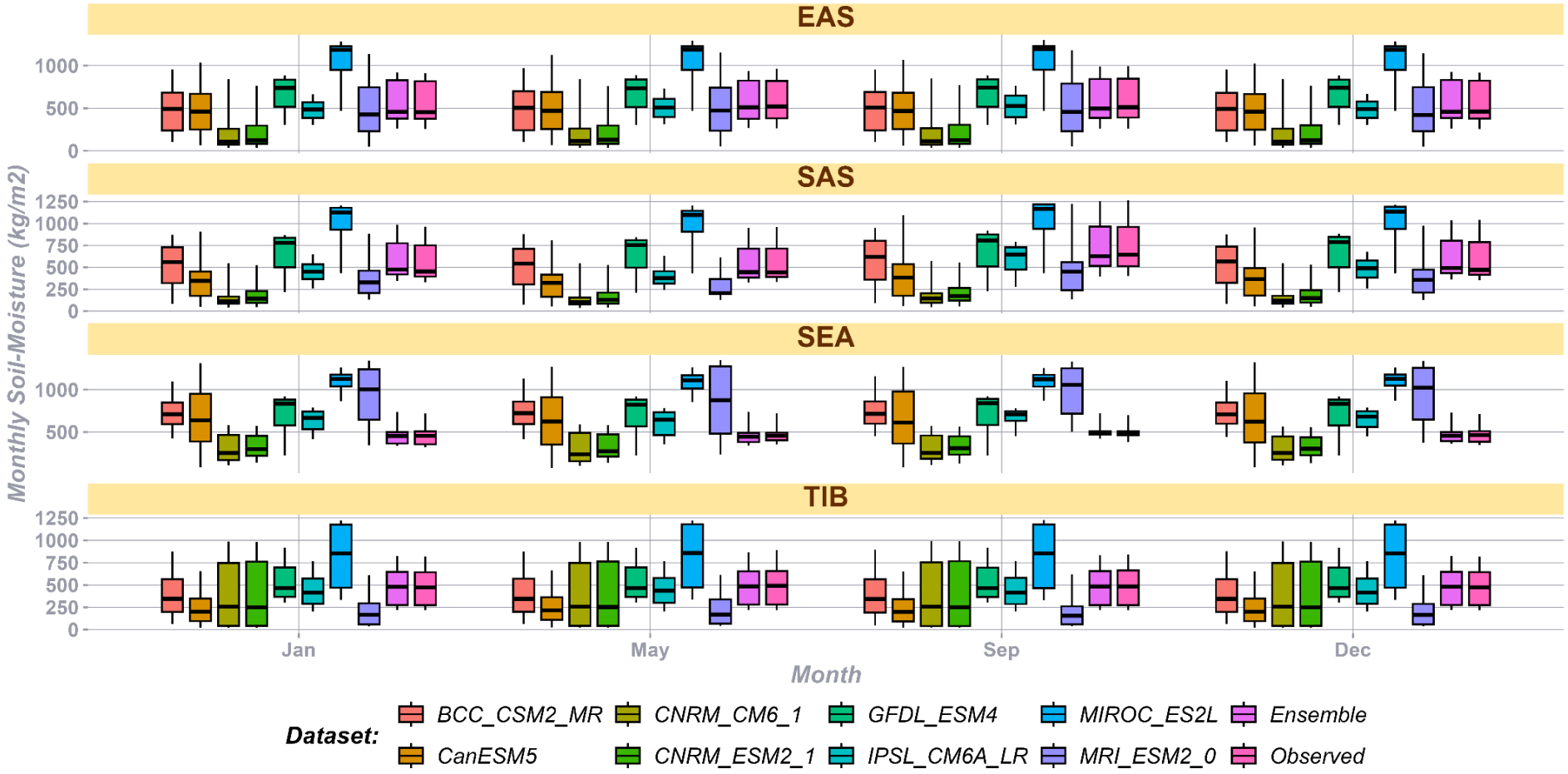

Figure S3: Monthly comparison of observed, ensembled, and individual climate model historical soil moisture data across four demarcated regions. Models with significant overestimation or underestimation are assigned lower weights through Bayesian Model Average (BMA).

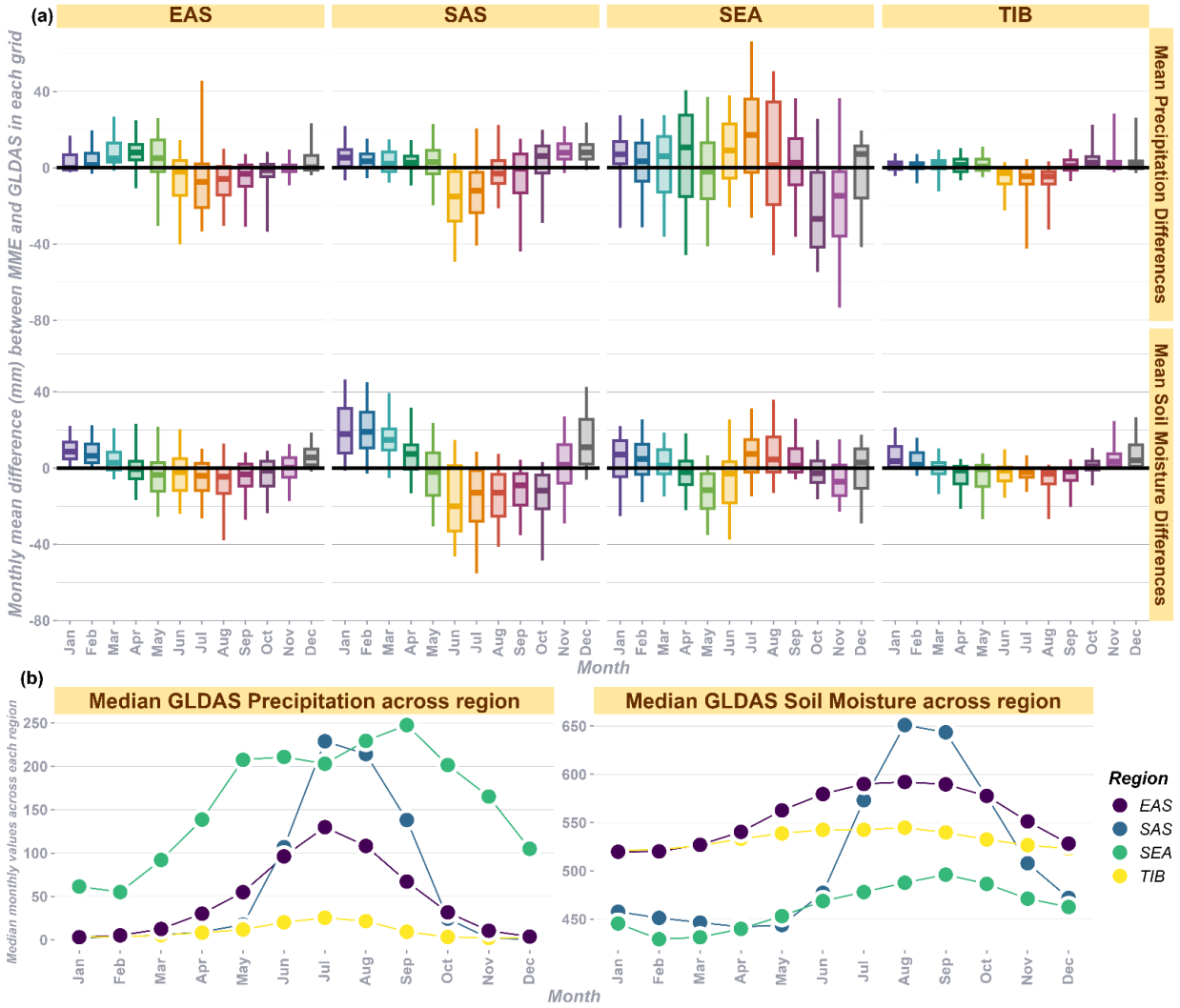

Figure S4: (a) Monthly distribution of the mean difference between GCM data (Multi-Model Mean using Bayesian Model Averaging) and GLDAS (Observed data) for precipitation and soil moisture, (b) Monthly median of observed precipitation and soil moisture data across four demarcated regions.

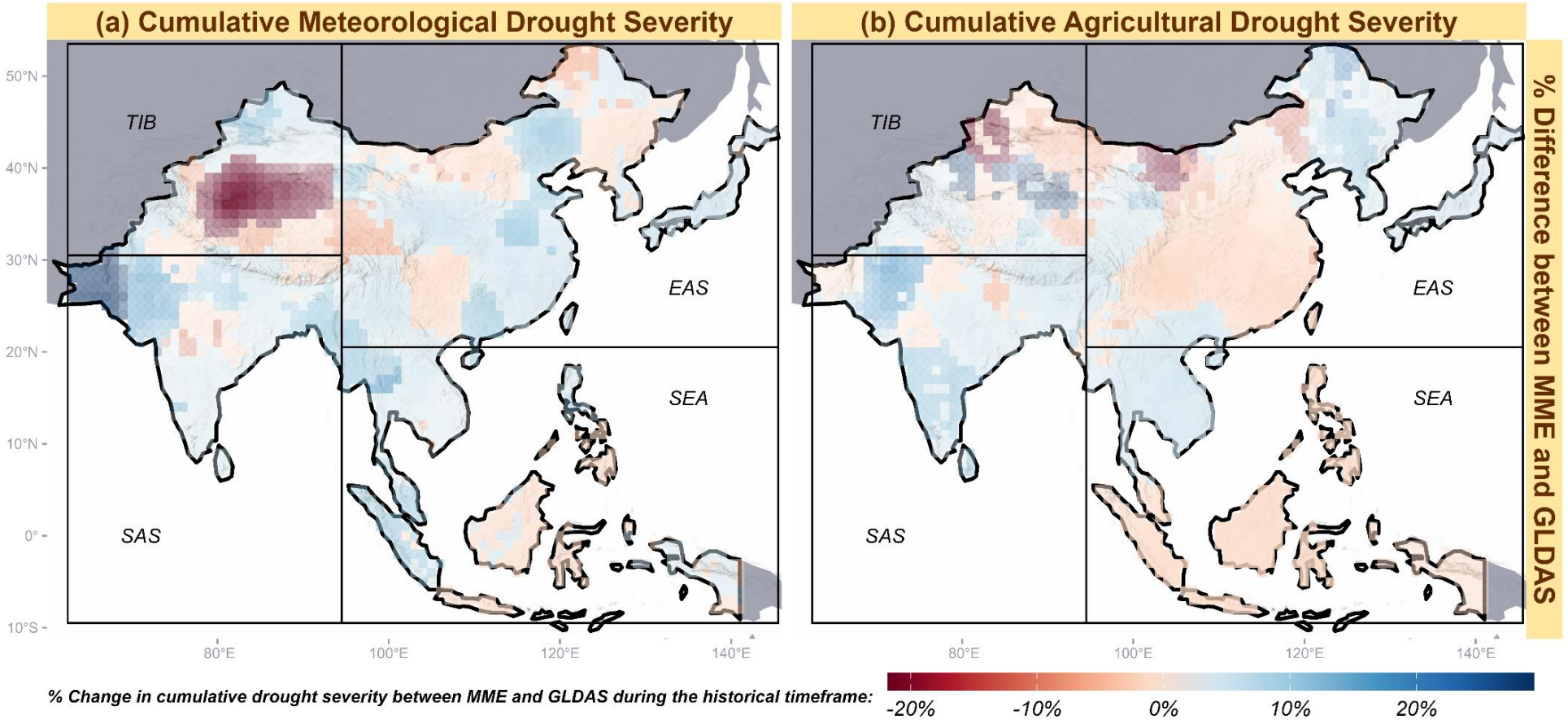

Figure S5: Differences in cumulative drought severities between the observed and historical MME for (a) meteorological and (b) agricultural droughts in the period between 1975-2014. Cumulative severity is the sum of index values below -0.5 in the period between 1975-2014 for each grid.

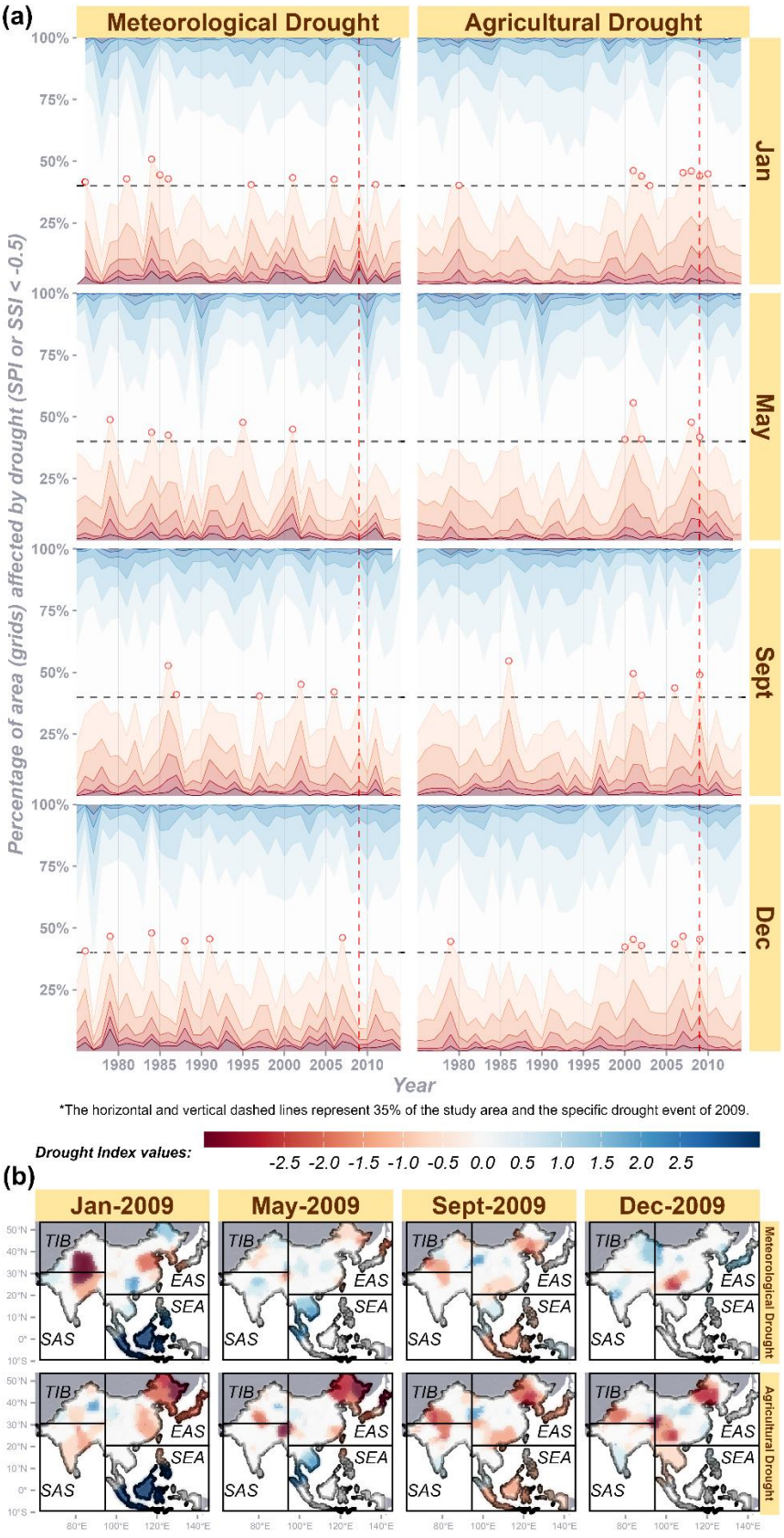

Figure S6: The percentage of drought-affected areas (based on the percentage of grids falling at different ranges of SPI and SSI values) annually. Spatial maps of 2009 drought events.

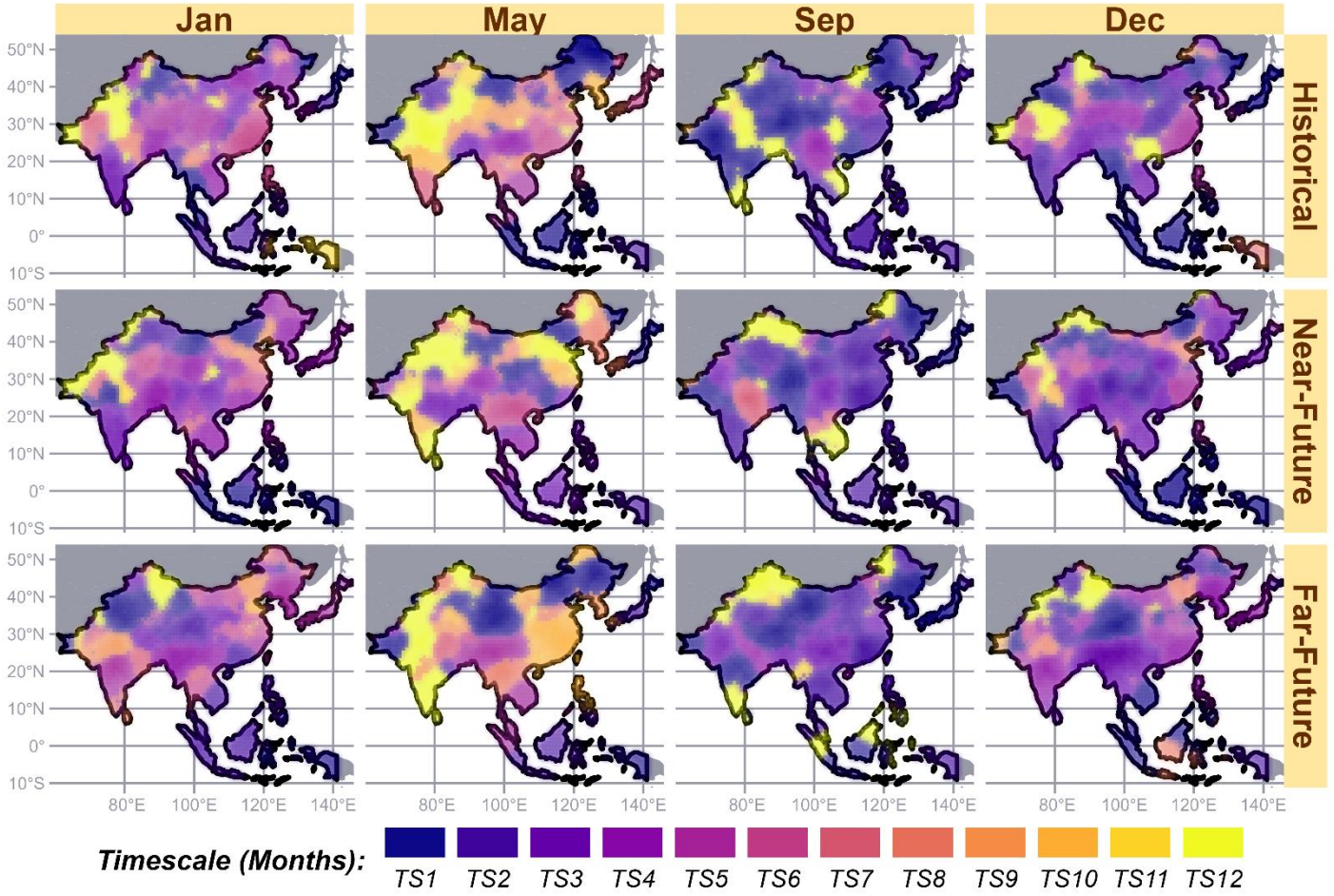

Figure S7: Spatial maps of propagation durations (timescale, TS) across different seasons and timeframes.

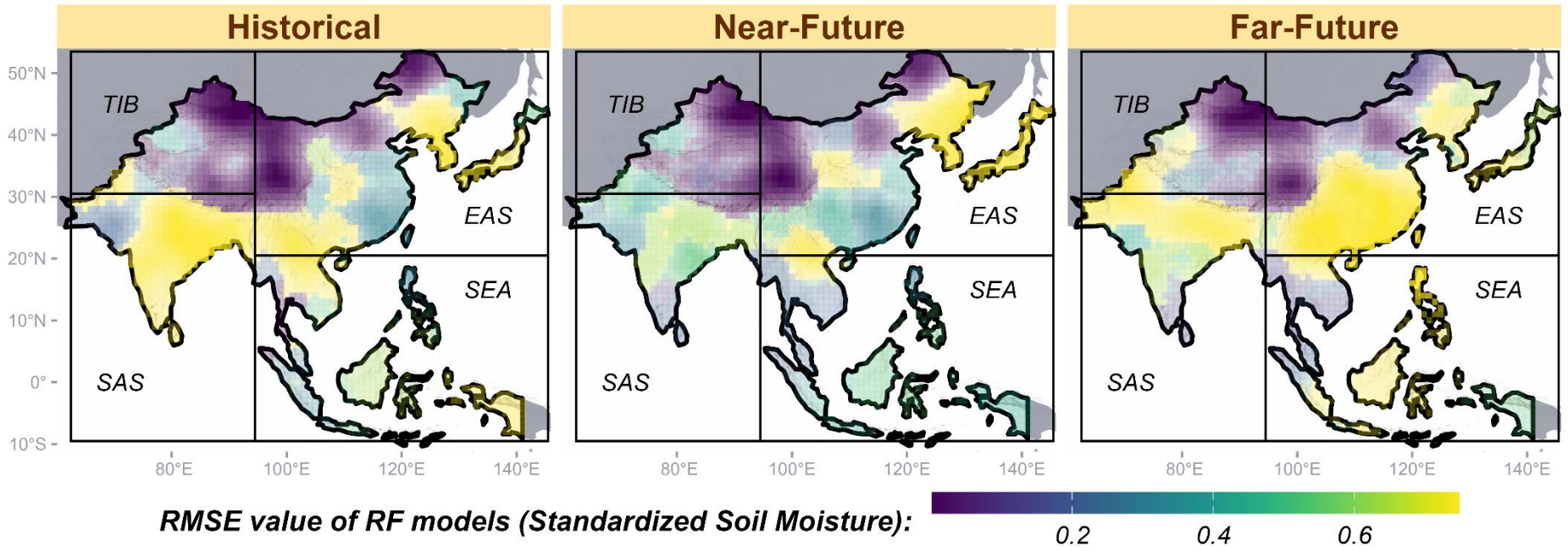

Figure S8: Performance evaluation (RMSE values) of Random Forest (RF) models for each grid across timeframes.

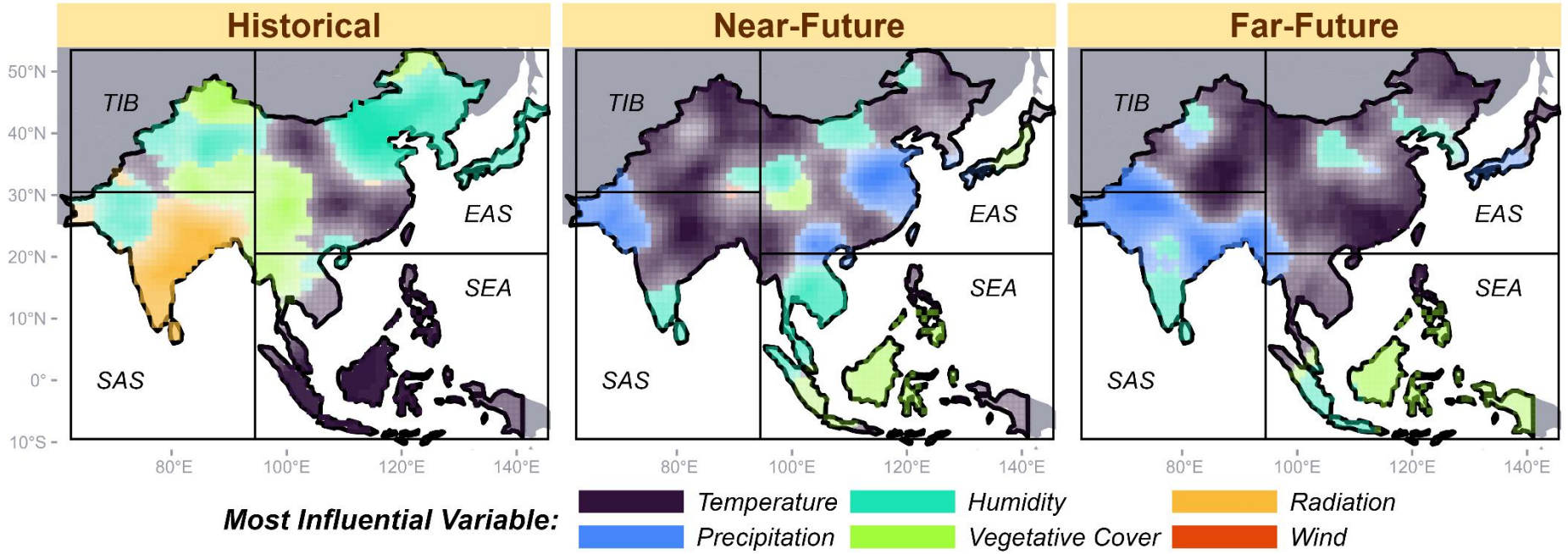

Figure S9: Maps showing the most important variable (highest importance value in a Random Forest model) across timeframes in the study area.

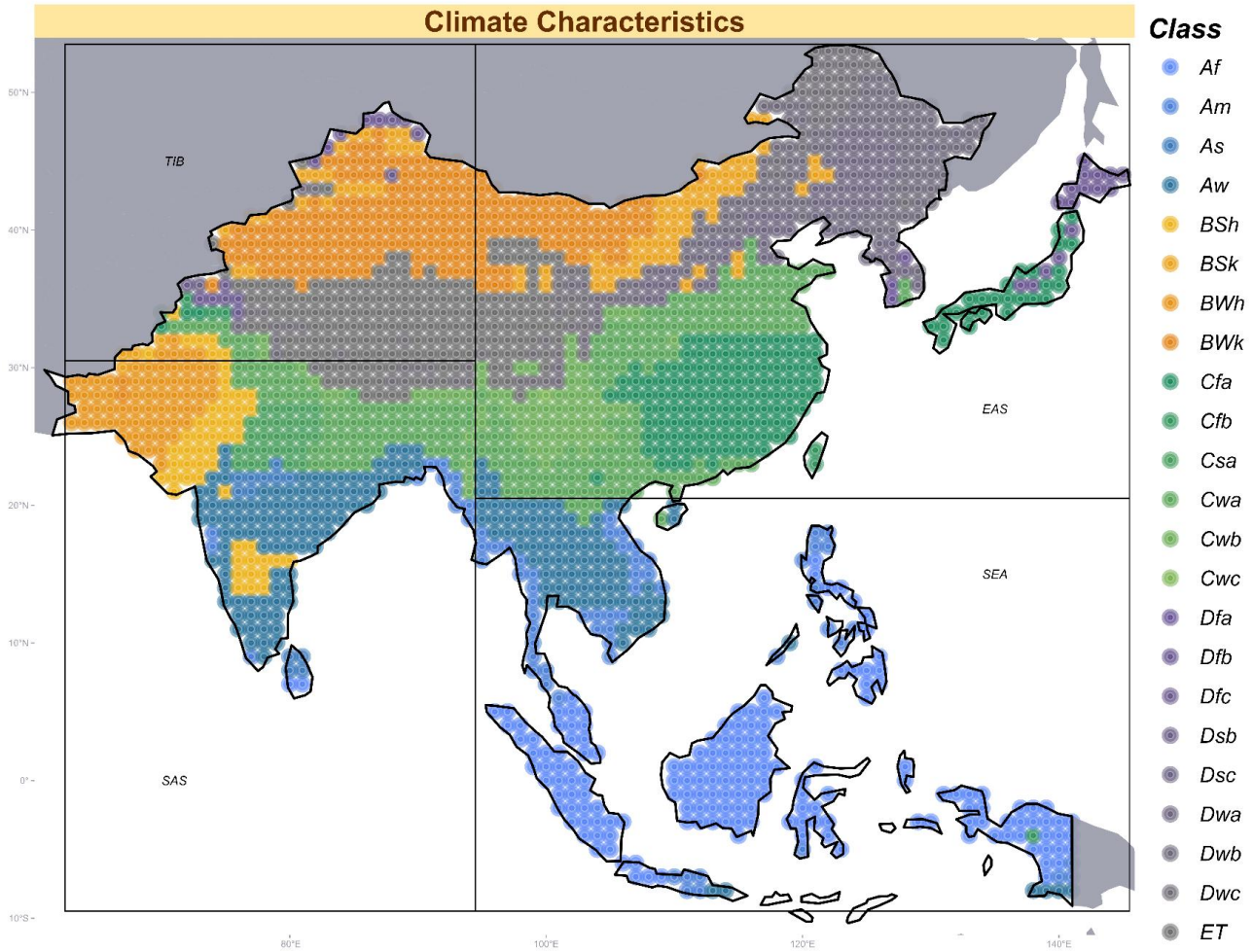

Figure S10: Climate zones based on the Köppen-Geiger climate classification (Kottek et al., 2006)

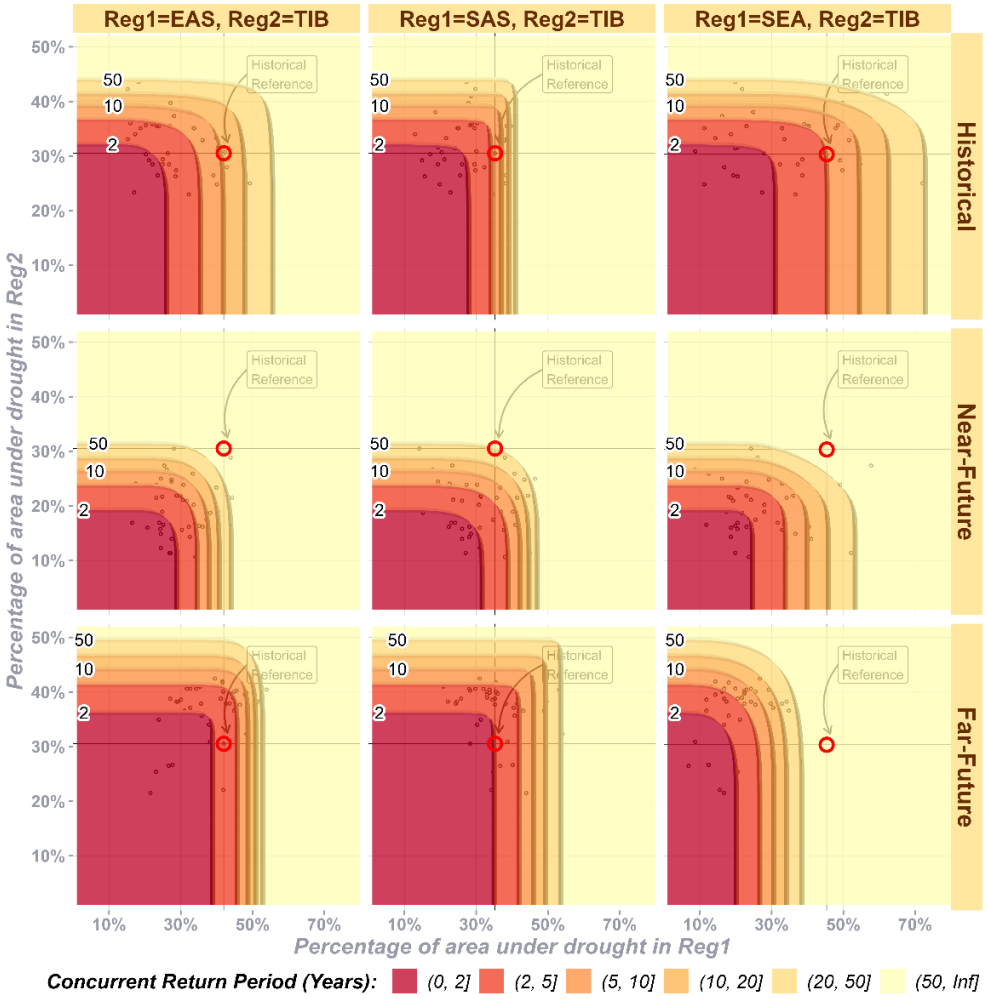

Figure S11: Spatial concurrent return period between region pairs involving TIB across timeframes. The random variables (percentage of area under drought annually) are shown as black dots.

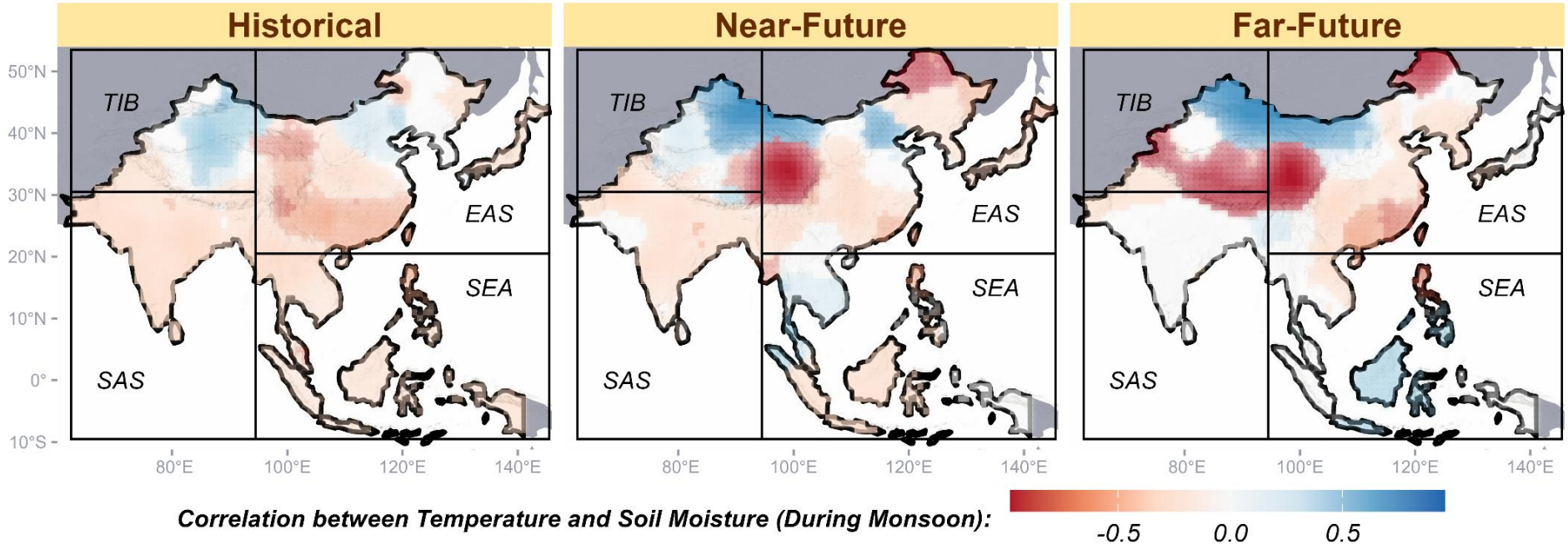

Figure S12: Correlation between temperature and soil moisture during monsoon season